von KARMAN INSTITUTE

FOR FLUID DYNAMICS

AFOSR 79-0033

LEVEL II

AN EXPERIMENTAL STUDY OF THE NOISE GENERATED BY A PUSHER PROPELLER DUE TO A WAKE ENTERING THE PROPELLER DISC

W. HERKES

November 5, 1979

Final Scientific Report, Nov. 1, 1978-Oct. 31, 1979.

Approved for public release; distribution unlimited

Prepared for : European Office of Aerospace Research
and Development
London, England

RHODE SAINT GENESE BELGIUM

REPORT DOCUMENTATION PAGE	READ INSTRUCTIONS BEFORE COMPLETING FORM
1. Report Number (18) (19) EDARD TR-80-5 / 2. Govt Accession No.	3. Recipient's Catalog Number (14) VKI-1979-17
4. Title (and Subtitle) (6) AN EXPERIMENTAL STUDY OF THE NOISE GENERATED BY A PUSHER PROPELLER DUE TO A WAKE ENTERING THE PROPELLER DISC	5. Type of Report & Period Covered Final Scientific Report Nov.1,1978-Oct.31,1979
	6. Performing Org. Report Number VKI Project Report 1979-17
7. Author(s) (10) W. Herkes / (12) 39 / (15) AFOSR	8. Contract or Grant Number 79-0033
9. Performing Organization Name and Address von Karman Institute for Fluid Dynamics Chaussée de Waterloo, 72 B-1640 Rhode Saint Genèse, Belgium	10. Program Element, Project, Task Area & Work Unit Numbers (16) 61102F 2301-01 (17) D1
11. Controlling Office Name and Address European Office of Aerospace Research and Development / LNV Box 14 FPO New York, 09510	12. Report Date November 5, 1979
	13. Number of Pages 36
14. Monitoring Agency Name and Address European Office of Aerospace Research & Development Box14 FPO New York, 09510	15. (11) 5 Nov 79
16. & 17 Distribution Statement Approved for public release; distribution unlimited.	
18. Supplementary Notes (9) Final rept. 1 Nov 78-31 Oct 79	
19. Key Words Pusher propellers; blade wake interference	
20 Abstract An experimental investigation of the noise gererated by a pusher propeller due to a wake entering the propeller disc was conducted. Acoustic measurements were made in a low speed wind tunnel with the propeller operating in a uniform velocity airstream, and with a wing mounted at various locations upstream of the propeller. For the propeller alone case the experimental results were compared with theoretical results.	

This report has been reviewed by the Information Office (EOARD/CMI) and is releasable to the National Technical Information Service (NTIS). At NTIS it will be releasable to the general public, including foreign nations.

This technical report has been reviewed and is approved for publication.

JOHN T. MILTON
Scientific and Technical Information Officer

ROBERT D. POWELL, Major, USAF
Chief, Flight Vehicles

FOR THE COMMANDER

GORDON L. HERMANN, Lt Colonel, USAF
Executive Officer

ACKNOWLEDGEMENTS

The author would like to express his gratitude to the numerous persons at the von Karman Institute who lent their assistance during the course of this investigation, and who made the author's stay at the vKI a very enjoyable one. Particular thanks are due to Dr. Roland Stuff and to Mr. Jean-Louis Hauchart. The author also wishes to acknowledge the Deutsche Forschungs and Versuchsanstalt für Luft und Raumfahrt and the Industrie Anlagen Beratungsgesellschaft for lending various pieces of experimental equipment and the United States Air Force for sponsoring this study.

ABSTRACT

An experimental investigation of the noise generated by a pusher propeller due to a wake entering the propeller disc was conducted. Acoustic measurements were made in a low speed wind tunnel with the propeller operating in a uniform velocity airstream, and with a wing mounted at various locations upstream of the propeller. For the propeller alone case the experimental results were compared with theoretical results.

TABLE OF CONTENTS

LIST OF FIGURES

LIST OF SYMBOLS

a	the local speed of sound
b	the frequency analyzer bandwidth
B	the number of blades
f	the rotational frequency of the propeller
J_n	the Bessel function of the 1^{st} kind of order n
m	the order of the sound pressure harmonic
M_e	the blade Mach number at the effective radius
O	an observation point in the Y=0 plane
Q	the total torque
R	the radial location of the blade element
R_b	the radius of the propeller
R_e	the effective radius of the propeller
R_o	the distance from the center of the propeller disc to O
R_u	the distance from a blade element to O
s	the blade loading harmonic number
SP_m	the root mean square sound pressure of the m^{th} sound pressure harmonic
SP_{m_s}	the root mean square sound pressure of the m^{th} sound pressure harmonic of the s^{th} blade loading harmonic
T	the total thrust
V	the wind tunnel velocity
X,Y,Z	coordinates of the fixed reference system
α	the wing angle of attack
α_s	the ratio of the s^{th} harmonic blade loading amplitude to the steady loading amplitude
δ	the angular location of O measured from the X axis
θ	the angular location of a blade element measured from the Z axis
Ω	the angular velocity of the propeller blade.

SECTION 1

INTRODUCTION

Pusher propeller aircraft are currently receiving considerable attention due to certain advantages which they display over tractor propeller aircraft. Because of its position behind a body, i.e., the fuselage or a wing, a pusher propeller operates in a lower velocity airstream, and thus more efficiently, than a tractor propeller. If, in the pusher propeller configuration, there is no part of the aircraft in the slipstream aft of the propeller, its efficiency is further improved. In addition, interest in laminar flow wings has encouraged engineers to study pusher propeller configurations, since such configurations do not produce disturbed air flows upstream of the wings.

However various disadvantages are associated with pusher propeller aircraft. Such designs generally involve locating the center of gravity further aft than in a comparable tractor design, thus decreasing the aircraft's stability. Also, particularly when it is mounted in the fuselage, there exists the problem that the propeller might strike the ground during take-off and landing. Additionally, due to the fact that a pusher's power plant is often located away from the oncoming airstream, engine cooling can become more difficult.

The purpose of the present investigation is to study still another difference between a tractor propeller and various pusher propeller configurations, that is, the difference in noise characteristics. Such differences are expected due to several effects of operating a propeller downstream of a solid body. First, due to the flow pattern around the body, the propeller operates in an airstream of nonuniform velocity. Second, the body produces a region of turbulent air flow in its wake, which

subsequently enters the propeller disc. Third, there is an inviscid interference between the aft body and the propeller blades. All these effects produce local incidence changes on the propeller blade, which in turn cause fluctuating forces on the blade, and thus additional noise sources. Several theories relevant to propeller noise generation are briefly presented in the following section.

The present investigation was conducted by suspending a wing upstream of a propeller in an open test section, low speed wind tunnel. A microphone, positioned outside of the moving airstream and connected to a frequency analyzer, was used to measure the sound pressure levels for different relative positions of the wing and propeller, as well as for the case of no wing being present. This experimental setup and procedure is described in more detail in Section 3. Finally, the results and conclusions of this study are presented in Sections 4 and 5.

SECTION 2

PROPELLER NOISE THEORY

2.1 The Theory of Lighthill

The noise generated by a rotating propeller is classified as aerodynamic noise, that is, noise generated by an air flow rather than by a vibrating solid. The classical theory of aerodynamic sound generation was first presented by Lighthill (1)[+]. He views his work as "uncovering the mechanism of conversion of energy between two of its forms, namely, the kinetic energy of fluctuating shearing motions and the acoustic energy of fluctuating longitudinal motions."

Lighthill considers a fluctuating fluid flow occupying a limited part of a large volume of fluid which is otherwise at rest. The exact equations governing the density fluctuations in the real fluid are compared to the linearized acoustic equation for the propagation of sound in a uniform medium at rest. He considers the difference between the two sets of equations as if it were the effect of a fluctuating external force field, known if the flow is known, acting on the acoustic medium, and therefore radiating sound in accordance with the ordinary laws of acoustics. In this manner Lighthill ultimately derives an expression governing the generation of aerodynamic sound.

2.2 The Theory of Gutin

The aerodynamic noise generated by a propeller can be classified as either discrete frequency 'rotational' noise or broad band noise. Discrete frequency noise arises from the regular, periodic disturbances of the air by the propeller. Broad band noise arises from random

---

[+]Numbers in parentheses refer to references listed at the end of the text.

disturbances at the propeller, such as those due to the fluctuating forces caused by vortex shedding from the trailing edges or by operating the propeller in a turbulent airstream. The present investigation is concerned with the more dominant discrete frequency noise.

The work of Gutin (2) forms the foundation of many current theories concerning propeller noise. Gutin considers the pressure distribution acting on an element of a propeller blade due to its motion through the air. He resolves this distribution into a thrust and a torque component. Since he considers the case of a uniform approaching air flow, these forces are steady in the rotating reference frame of the propeller. However, at a fixed point in space the forces on this element appear as oscillating forces, the frequency of oscillation being equal to the rotational frequency of the blade element. This situation is depicted in Figure 1 in which

X,Y,Z define the fixed coordinate system

O = an observation point in the Y=0 plane

Ω = the angular velocity of the propeller blade

R_b = the radius of the propeller

R_o = the distance from the center of the propeller disc to O

R_u = the distance from a blade element to O

R = the radial location of a blade element

θ = the angular location of a blade element measured from the Z axis

R dR dθ = a blade element

δ = the angular location of O measured from the X axis

dQ = the torque produced by a blade element

dT = the thrust produced by a blade element

Since the excitation is periodic, it can be Fourier analyzed and the harmonics considered separately. Gutin assumes the blade width to be

small enough that the excitation can be treated as an impulse function, then develops expressions for the varying thrust and torque forces for each harmonic. He proceeds with the mathematics and ultimately derives an integral expression for the sound pressure of each harmonic. In order to solve this equation exactly the thrust and torque distributions along the propeller radius must be known. However, Gutin obtains an approximate solution by assuming an effective radius at which the total thrust and torque are assumed to act. His final expression[+] is

$$SP_m = \frac{m\,B\,\Omega}{2\pi\,a\,R_0}\left(-T\cos\delta + \frac{Q}{R_e\,M_e}\right) J_{mB}(m\,B\,M_e\sin\delta)$$

where

m = the order of the sound pressure harmonic

B = the number of blades

SP_m = the root mean square sound pressure of the m^{th} sound pressure harmonic

a = the local speed of sound

T = the total thrust

Q = the total torque

R_e = the effective radius of the propeller

M_e = the blade Mach number at the effective radius

J_{mB} = the Bessel function of the 1^{st} kind of order mB

It can be seen that the thrust contribution has a quadrapole-type directivity character, while the torque has a dipole-type directivity character. The signs of the thrust and torque contributions indicate whether they are in phase, and thus constructive, or out of phase, and thus destructive. These directivity characteristics are shown in Figure 2.

In general, a dipole is a much more effective radiator than a

---

[+]For the sake of consistency, the author has taken some liberty with the original notation in this and other expressions.

quadrapole. In the case of a propeller, however, since the thrust force is significantly greater than the torque force, these two contributions to the sound pressure are of comparable magnitude. The magnitude of the contribution due to the finite thickness of the propeller blade, which Gutin does not consider, is comparable to the magnitudes of the torque and thrust contributions only at relatively high blade tip Mach numbers. Also not considered by Gutin is the contribution of broad band noise such as vortex shedding noise. Under most operating conditions, the effect of broad band noise on the discrete frequency sound pressure levels is insignificant. Another assumption of Gutin is that the forward speed of the propeller is low enough that it does not affect the directivity or the amplitude of the sound pressures.

It is worth noting the effect of the Bessel function term on the theoretical sound pressure. For relatively small values of (M_c sinδ) the amplitudes of the harmonics decrease with harmonic number. However, the rate with which the harmonic amplitude increases with (M_c sinδ) is greater for higher order harmonics. Thus for relatively large values of (M_c sinδ) these higher order harmonics can assume larger values than the lower order ones.

2.3 The Theory of Wright

Wright (3) considers a propeller operating in a nonuniform flow field, i.e., one in which the angle of incidence on the propeller blade varies as the blade rotates. This, of course, is the situation arising when the wake produced by an upstream body enters the propeller disc. Under such conditions a fluctuating force field exists on the propeller blade in the rotating reference frame.

Wright considers the case in which these force fluctuations are repetitive for each revolution (stationary asymmetric disc loading), and

thus can be Fourier analyzed into blade loading harmonics. These harmonic components can be realized as a distribution of sinusoidally oscillating forces, rotating with the blade. Thus, he concludes, at a fixed point in space each blade loading harmonic produces a spectrum of fluctuating forces. This spectrum consists of a force fluctuating at the blade passage frequency and of forces fluctuating at side-band frequencies occurring at multiples of the blade passage frequency. Associated with these fluctuations are the relatively efficient dipole sound sources. Thus when these force fluctuations are large their contribution to the sound pressure spectrum is also large.

The overall spectrum of sound pressure harmonics is, therefore, the sum of the sound pressure spectrums of each blade loading harmonic. Using this model for stationary asymmetric disc loading, Wright ultimately derives the following simplified expression:

$$SP_{m_s} = \frac{a_s\, m\, B\, \Omega}{2\,\pi\, a\, R_o}\ (-T\cos\delta + \frac{Q}{R_c\, M_c}$$

$$(\frac{m\,B - s}{m\,B})\ )\ \ J_{mB-s}\ (m\,B\,M_c\sin\delta)$$

where

s = the blade loading harmonic number

SP_m = the root mean square sound pressure of the m^{th} sound pressure harmonic of the s^{th} blade loading harmonic

a_s = the ratio of the s^{th} harmonic blade loading amplitude of the steady loading amplitude

It can be seen that for the case of steady disc loading, i.e., $s=0$ and $a_{s=0}=1$, the above equation reduces to that of Gutin. As is the case with Gutin's equation, Wright's equation does not consider the effects of forward speed, thickness or broad band noise, or the pressure distributions along the blade. It should be noted that in Wright's equation the

Bessel function term has the same argument, but a different order than in Gutin's equations. Thus the relative amplitudes of the harmonics are not dependent only upon ($M_e \sin\delta$), but also upon s.

SECTION 3

EXPERIMENTAL SETUP AND PROCEDURE

3.1 Experimental Setup

The present investigation of the noise generated by an aircraft propeller and the effect of an upstream wing on this noise generation was conducted in the von Karman Institute (vKI) low speed wind tunnel L-1 (4). The overall test setup is shown in Figures 3 and 4.

An open-jet test section having a diameter of 3 meters and a jet length of 4.6 meters was used. As the wind tunnel was not designed to be used for acoustic measurements, its acoustic qualities were improved by placing closed cell polyurethane foam (Eurofoam quality LF) sheets, 4 cm thick, in various locations. In order to reduce reflections, this foam was hung behind the test section and was applied to the control room, to a support column, and to the underside of the overhead balance. It was also used to dampen the noise from the propeller engine generator.

The propeller used in this study was borrowed from the Industrie Anlagen Beratungsgesellschaft (IABG) and is shown in Figure 5. It is a two bladed propeller of simple design, constructed of laminated wood, and measuring 347 mm in diameter. The propeller was powered by a 3-phase electric engine, belonging to the Deutsche Forschungs und Versuchsanstalt fUr Luft und Raumfahrt (DFVLR). This engine was mounted in a casing containing a water-supplied cooling coil. An adapting cone was designed and fabricated at the vKI to connect the propeller to the engine shaft. The engine, propeller, and cooling casing were suspended from the overhead 6-component mechanical balance, as shown in Figure 6, in such a way that the torque and thrust produced by the propeller could be measured.

The wing used in this investigation was a symmetric RAE 101 profile wing belonging to the DFVLR, having a chord of 300 mm and a span of

1800 mm. It was supported from below in such a way that both its horizontal and vertical positions could be varied. All tests were done with the wing positioned at a geometric angle of attack of -8^{o}, the results being applicable to a wing at $+8^{o}$ due to its symmetry. Figures 4 and 7 show two views of a propeller/wing configuration.

It is important to note the coordinate system used throughout this report. The origin is at the center of the propeller disc, the X axis is directed upstream, and the Y axis downward. The relative location of the wing to the propeller is defined by the location of its trailing edge in this coordinate system.

The acoustic measuring and recording equipment used was manufactured by Brüel and Kjaer. This equipment consisted of a type 4133 12.7 mm condenser microphone and preamplifier, a type 2120 frequency analyzer, a type 2307 level recorder, and a discrete frequency calibrator. The microphone was mounted at the height of the center of the propeller disc, 3 meters from the propeller, and at an angle of 70^{o} from the approaching airstream. This location was based on preliminary estimates of the far field and on previous far field studies done in the L-1 wind tunnel (5).

3.2 Experimental Procedure

The general test procedure can be summarized as follows:

1. start water flow to propeller engine cooling casing
2. calibrate acoustic equipment
3. position microphone
4. position wing
5. start wind tunnel
6. start propeller engine
7. make acoustic measurements
8. make torque and thrust measurements
9. shut down propeller engine
10. shut down wind tunnel
11. repeat steps 4 through 10 for a different propeller/wing configuration, periodically recalibrating the acoustic equipment

The only parameters varied in the present study were the X and Y locations of the wing. All other parameters were held constant as indicated below:

microphone location: $\delta = 70^{o}$

$R_{o} = 3$ m

$Y = 0$ m

tunnel operating condition: $V = 30\ (\pm\ 1)$ m/s

propeller operating condition: $f = 200$ Hz

wing angle of attack: $\alpha = -\ 8^{o}$

frequency analyzer bandwidth: $b = 10\%$

SECTION 4

RESULTS AND DISCUSSION

4.1 Preliminary Results

Before making measurements of the noise generated by the propeller several preliminary tests were performed. First a calibration check was performed on the torque and thrust balances. While the thrust balance functioned satisfactorily, problems were encountered with the torque balance. Therefore, in this study the torque is calculated on the basis of the power used by the propeller engine, assuming an appropriate efficiency coefficient.

A wake survey was made at various locations downstream of the wing using a pitot-static probe rake. The results of this survey appear in Figure 8. It must be noted, however, that these profiles do not take into account the suction effect of the propeller. This effect must be considered when attempting to determine where the wake is actually entering the propeller disc.

The quantities of interest in this study are the amplitudes of the sound pressures at the harmonic frequencies. Thus a narrow band spectral analysis is desirable. A test was performed, with the propeller operating, to compare the results of using a 10%, as opposed to a 1%, bandpass width. Since the difference between the two cases was negligible, the 10% bandpass filter was used, as this analysis requires less time.

4.2 Propeller Alone Results

Before studying the effect of the presence of the wing on the propeller generated noise, a spectral analysis was performed on the noise generated by the propeller in a uniform velocity airstream. The result of this analysis is shown in Figure 9. In this figure the base line

represents a sound pressure level of 80 dB (referenced to 20 $\mu N/m^2$), and the horizontal lines are spaced 2 dB apart. The graph covers a frequency range of 250 to 2500 Hz. Since the propeller was rotating at 200 revolutions per second and has two blades, its fundamental frequency was 400 Hz.

At this point it should be mentioned that zero shifts of the frequency analyzer of as much as 1 dB were experienced in the course of testing. Thus the results presented in this report have at least that level of uncertainty.

For the propeller alone test the values of the torque and thrust (i.e., Q=0.18 N·m and T=0.63 N) and of the other necessary parameters were inserted into Gutin's expression for the theoretical sound pressure. The resulting values, expressed in terms of decibel levels, are shown graphically in Figure 10 for the first five harmonics. The theoretical values at $\delta=70^{\circ}$, i.e., at the microphone location, are shown in Figure 11, plotted with the measured values. As can be seen, the agreement is not satisfactory, particularly for the first two harmonics for which the trend of the amplitudes is reversed. Thus various possible explanations for the lack of agreement were considered.

Since there was no sound absorbing material on the floor, the effect of a reflection off the floor was investigated. The concrete floor was assumed to be a perfect reflector and the propeller was treated as a point sound source located at the center of the propeller disc. The computed amplification factors for the first five harmonics for various source-to-receiver distances are shown in Figure 12. Applying these factors to the measured data for the nominal source-to-receiver distance of 3 meters gave unsatisfactory results. However, for a source-to-receiver distance of 2.9 meters, the correction factors gave good agreement for the first two harmonics, as shown inFigure 11. It is quite possible that

during the course of testing the microphone stand had been misplaced or incorrectly measured by 10 cm. While it was not possible at this point to check the actual source-to-receiver distance, the improved agreement of the first two harmonics and the conceivable explanation appear to justify the assumption of a source-to-receiver distance of 2.9 meters.

This reflection correction, however, failed to resolve the discrepancy between theory and measurement for the higher order harmonics. Goldstein (6) cites a similar reported discrepancy and attributes the additional high frequency noise, unpredicted by Gutin's theory, to non-uniform flow entering the propeller disc. The validity of Gutin's assumption of an effective radius to model the higher order harmonics has been questioned, and could also contribute to the discrepancy. Other factors that could have been influencing the experimental results include the diffraction effect of the shear layer of the open-jet and the presence of additional untreated reflecting surfaces in the test area.

4.3 Propeller/Wing Results

A series of tests was performed to study the effect on the noise generation of varying the vertical location of the wing. For these tests the horizontal location of the wing was held constant at X=250 mm. The results of these tests are shown in Figure 13. This figure indicates the spectral sound pressure levels for various Y locations of the trailing edge of the wing. The figure shows an envelope of the sound pressure levels, that is to say, only the amplitudes at the harmonic frequencies reflect measured values. The values at these frequencies are simply connected by straight lines and thus amplitudes at intermediate frequencies cannot be inferred from this graph. When viewing this graph it should be noted that the radius of the propeller is 173.5 mm and the radius of the cone is 32.5 mm. However, as mentioned earlier, the exact location where the wake enters the propeller disc is uncertain.

The most noticeable trend is that the amplitude of the second harmonic tends to be the greatest for most propeller/wing configurations. Both the fundamental and the fifth harmonic increase somewhat with Y; however, it is unclear whether this is indicative of a significant trend. It is not known why the values at Y=395 mm, where the wake certainly does not enter the propeller disc, differ from the case of the propeller alone (See Figure 9.).

The correction factor for the ground reflection was applied to the data and these results are shown in Figure 14. This correction eliminates the trend of the second harmonic to have the highest sound pressure level.

Figure 15 shows the overall sound pressure levels for various propeller/wing configurations for both the uncorrected and the corrected data. There appears to be an increase in sound pressure with increasing horizontal location of the wing for the corrected data. However, the large scatter makes this trend questionable.

Another correction could be applied to the data by using the correction factors necessary to bring the wing alone data into agreement with Gutin's theory. Such a correction would result in a much more rapid decrease of the spectral sound pressure levels with increasing harmonic number.

Another series of tests to study the effect of changing the vertical location of the wing was performed, this time for a horizontal location of X=100 mm. However, for this series the repeatability was so poor, particularly when the wing was near the propeller cone, that no meaningful data could be obtained. The cause of this irrepeatability is uncertain, but an unsteadiness of the wake impinging on the cone is possible. The fact that such an unsteadiness did not appear when the wing was at a horizontal location of X=250 mm may be due to the fact that the wake is much weaker with the wing at that location. This could

also explain why no strong trends appeared for the X=250 mm case as the vertical location of the wing was varied.

A series of tests was conducted to test the effect of changing the horizontal location of the wing. Again a large degree of irrepeatability was encountered. However, despite this irrepeatability, an increase of the overall sound pressure level was obvious as the wing was moved quite close to the propeller.

SECTION 5

CONCLUDING REMARKS

More than anything else, this investigation indicates the need for further study of the effect of a wake on the noise generated by a propeller. The experimenter must be able to have confidence that his measurements are truly indicative of the propeller generated noise. In the case of the vKI L-1 wind tunnel this requires a close examination of the reflective and diffractive characteristics of the tunnel and test area. Based on this examination, either the acoustic character of the tunnel or the experimental data could be suitably corrected.

A detailed study of the wake and the propeller/wake interaction is essential in order to be able to relate the noise measured to the flow phenomena producing it. Knowledge of the wake character, coupled with improved experimental technique, would help resolve whether the unsteadiness encountered in the present study is indicative of an unsteadiness of the flow itself. Knowledge of the propeller/wake interaction is also required in order to compare the theoretical and the experimental results.

Finally, more extensive testing is necessary. This should include variation of the microphone location, as well as other test parameters.

REFERENCES

1. Lighthill, M. J.: "On Sound Generated Aerodynamically, I. General Theory," Proc. Roy. Soc., Ser. A. vol. 211, 1952, pp. 564-587.

2. Gutin, L.: "On the Sound Field of a Rotating Propeller," NACA TM 1195, 1948.

3. Wright, S. E.: "Sound Radiation from a Lifting Rotor Generated by Asymmetric Disk Loading," J. Sound Vib., 9(?), 1969, pp. 223-240.

4. Colin, P. E.: "The Low Speed Tunnel L-1," TCEA TM 8, 1960.

5. Oetting, R. B.: "Preliminary Noise Measurements in the Open-Jet of the vKI Low Speed Wind Tunnel, L-1," vKI TN 89, 1973.

6. Goldstein, M." Aeroacoustics, NASA SP-346, 1974. (Also McGraw-Hill, 1976.)

General Reference: Richards, E. J. and Mead, D. J.: Noise and Acoustic Fatigue in Aeronautics, John Wiley and Sons, Ltd., 1968.

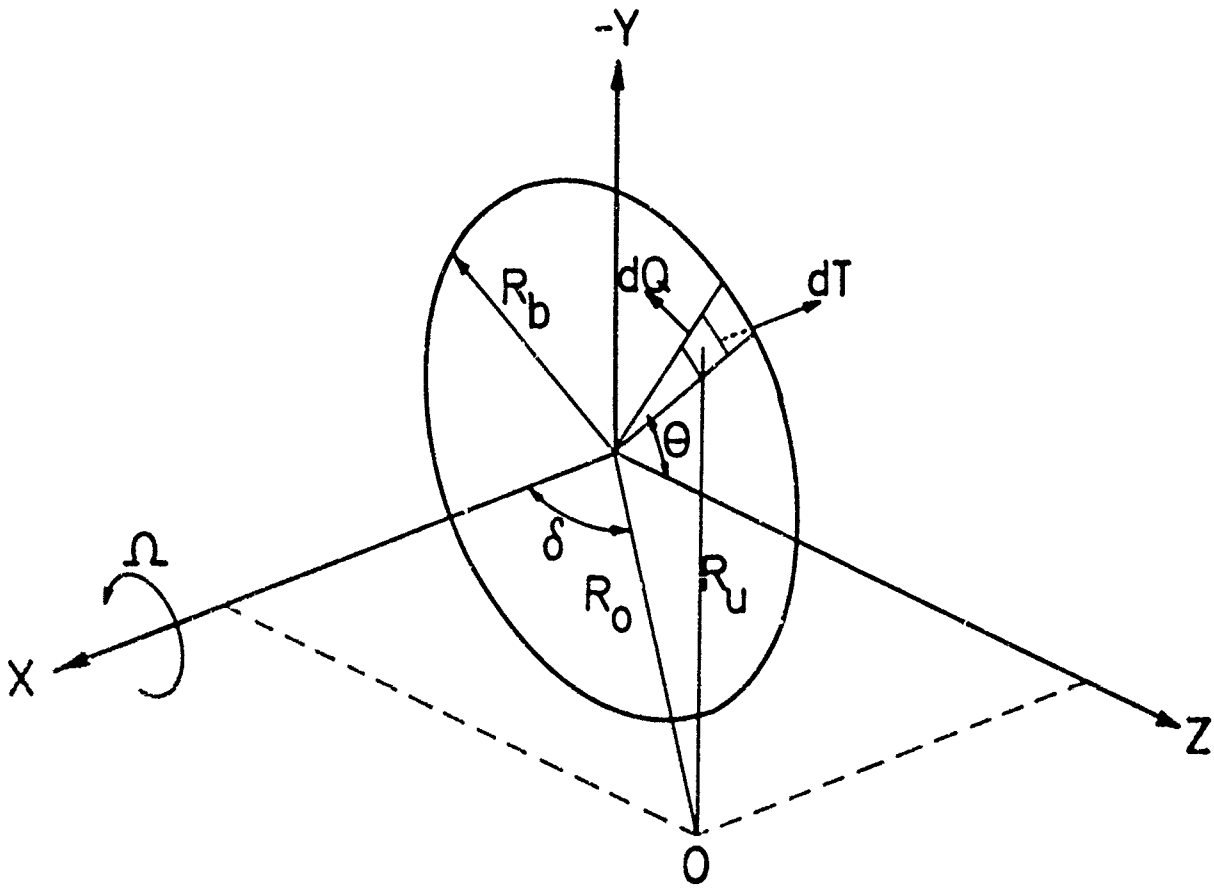

FIGURE 1: SCHEMATIC DIAGRAM OF THE PROPELLER DISC

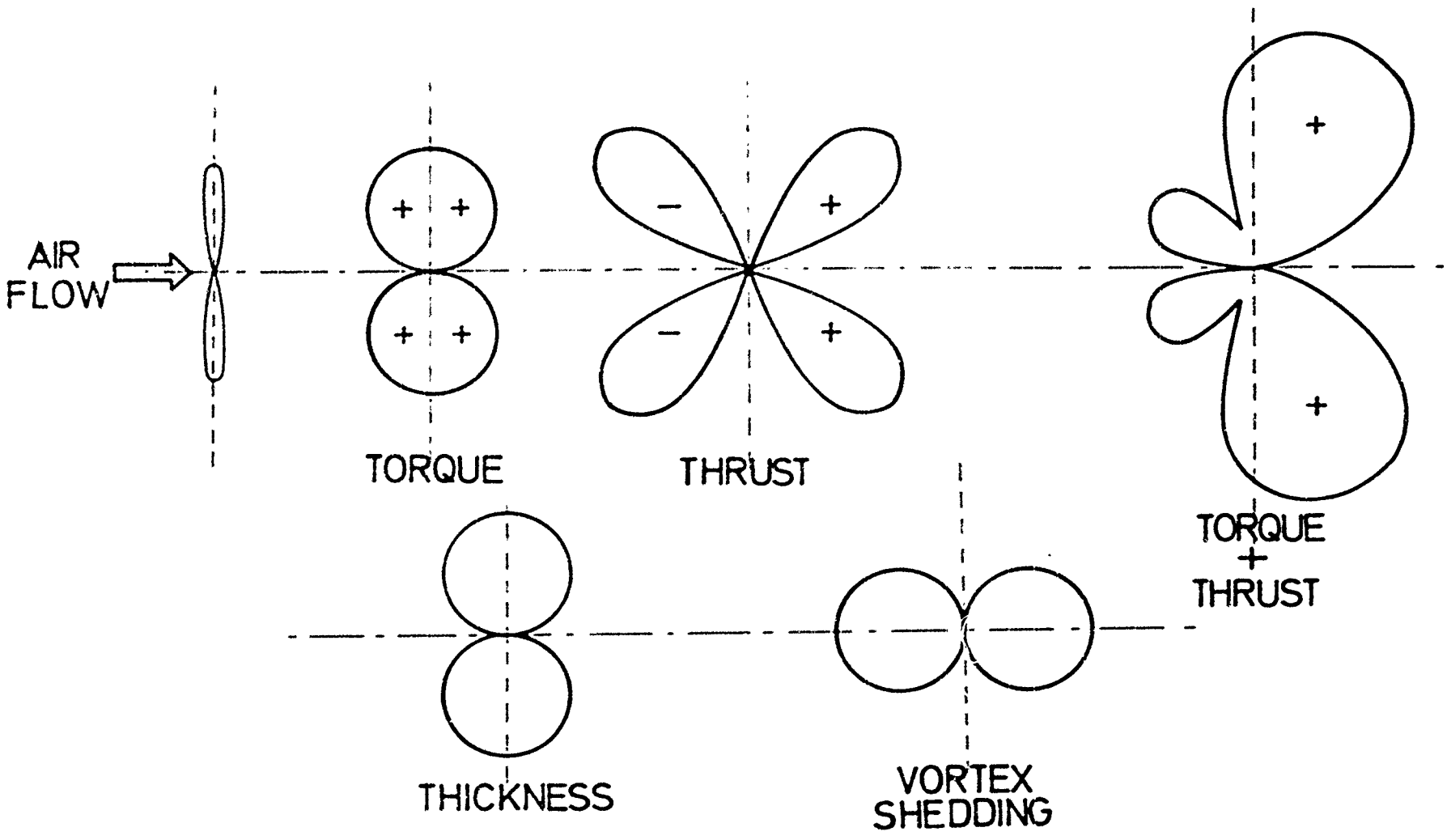

FIGURE 2: DIRECTIVITY PATTERNS FOR VARIOUS NOISE SOURCES

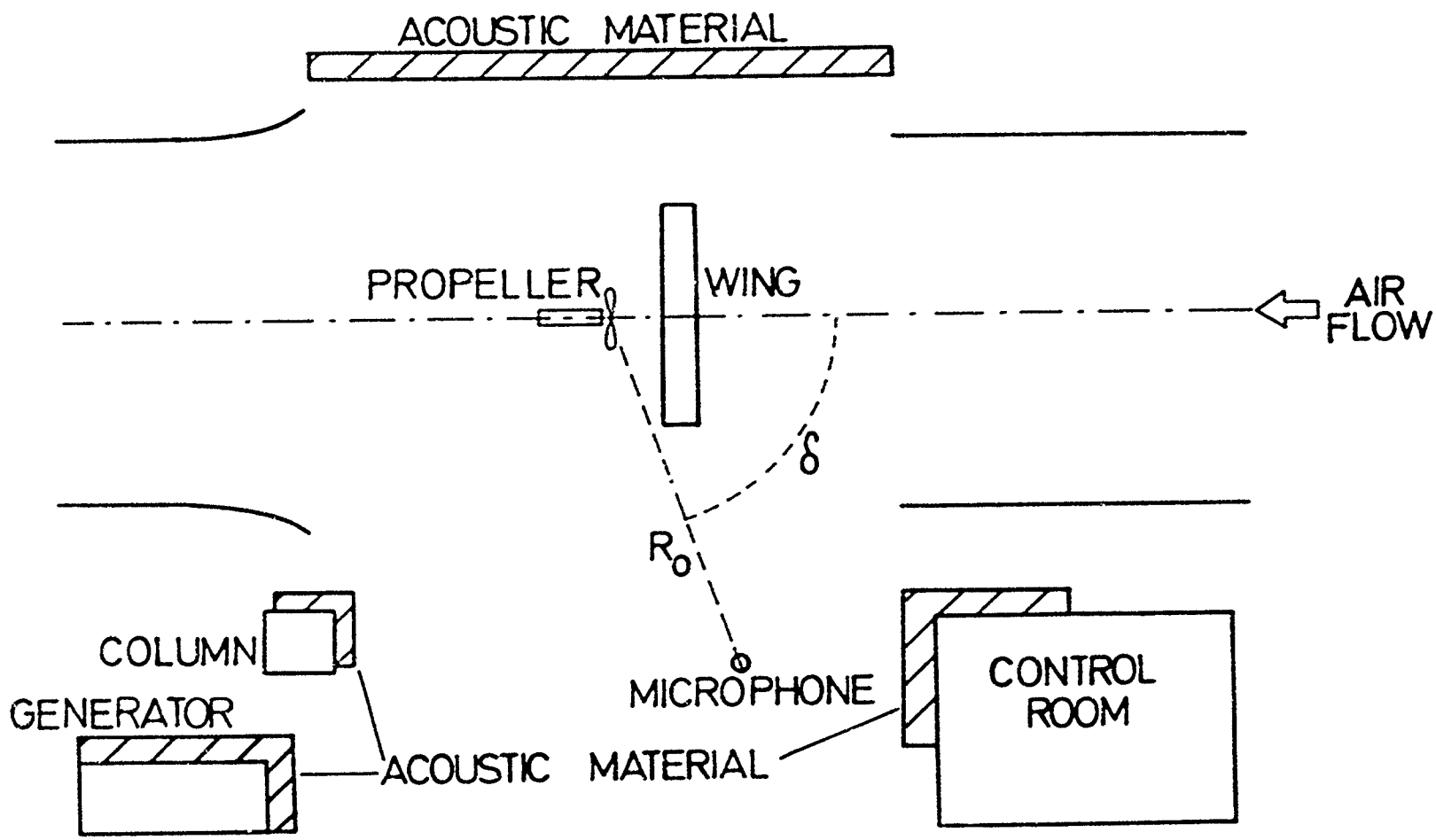

FIGURE 3: SCHEMATIC DIAGRAM OF THE OVERALL TEST SETUP

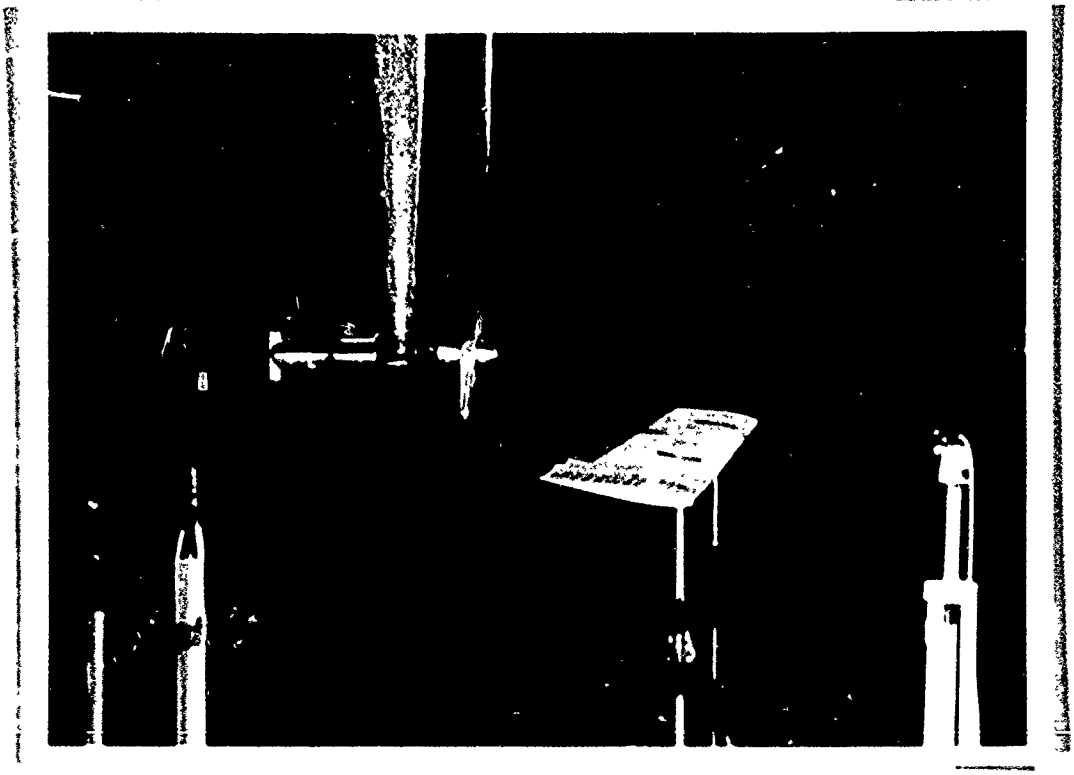

FIGURE 4: PHOTOGRAPH OF THE OVERALL TEST SETUP

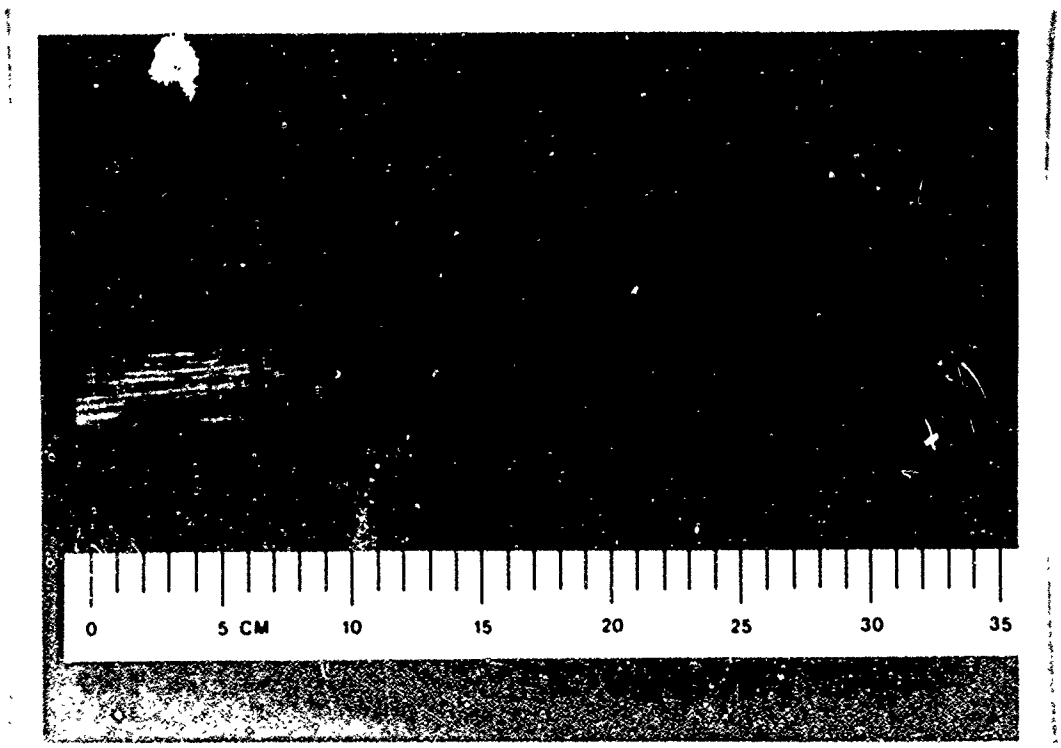

FIGURE 5: PHOTOGRAPH OF THE PROPELLER

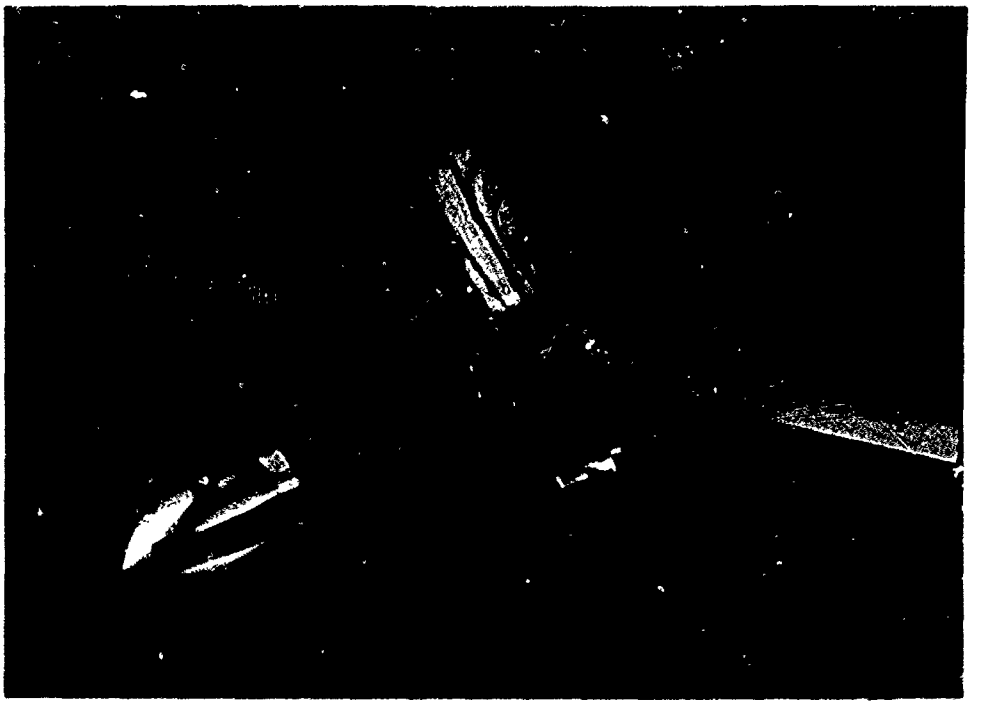

FIGURE 6: PHOTOGRAPH OF THE PROPELLER, ENGINE, AND COOLING CASING

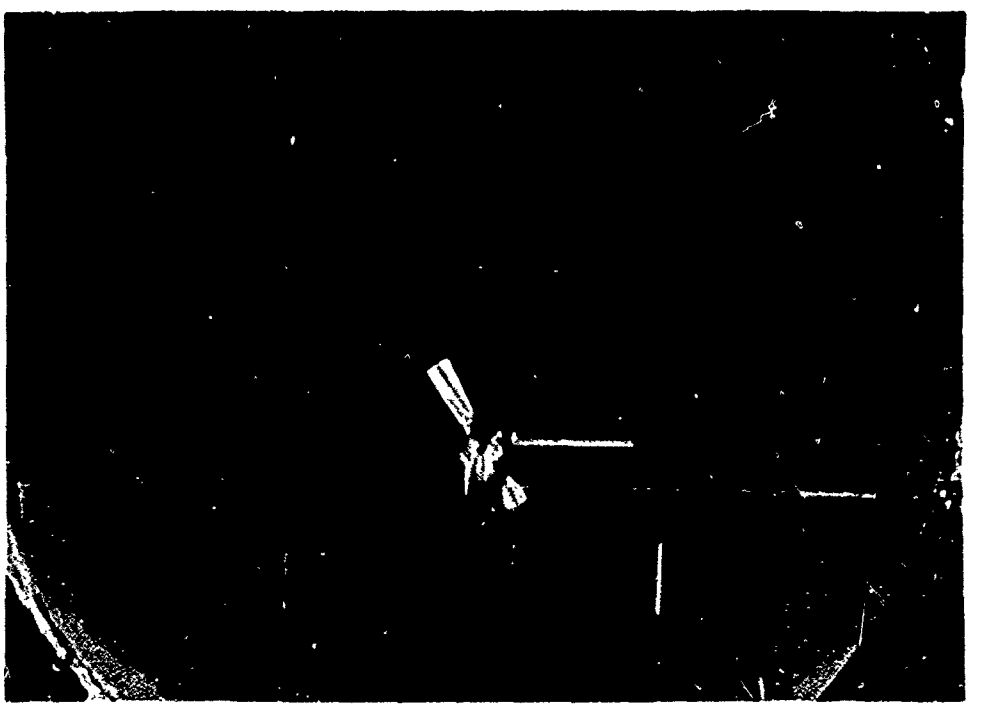

FIGURE 7: PHOTOGRAPH OF THE PROPELLER/WING CONFIGURATION LOOKING UPSTREAM

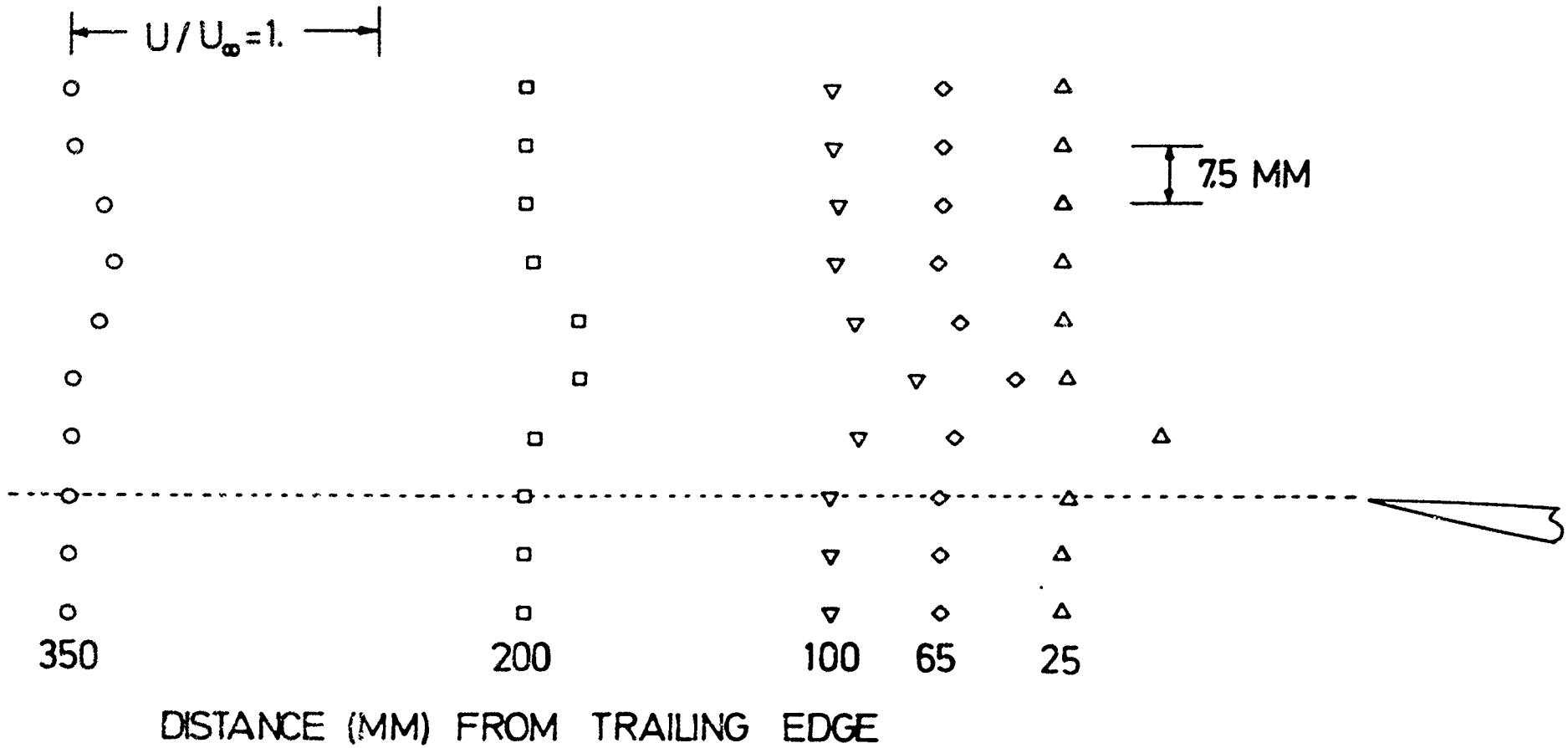

FIGURE 8: WING WAKE PROFILES

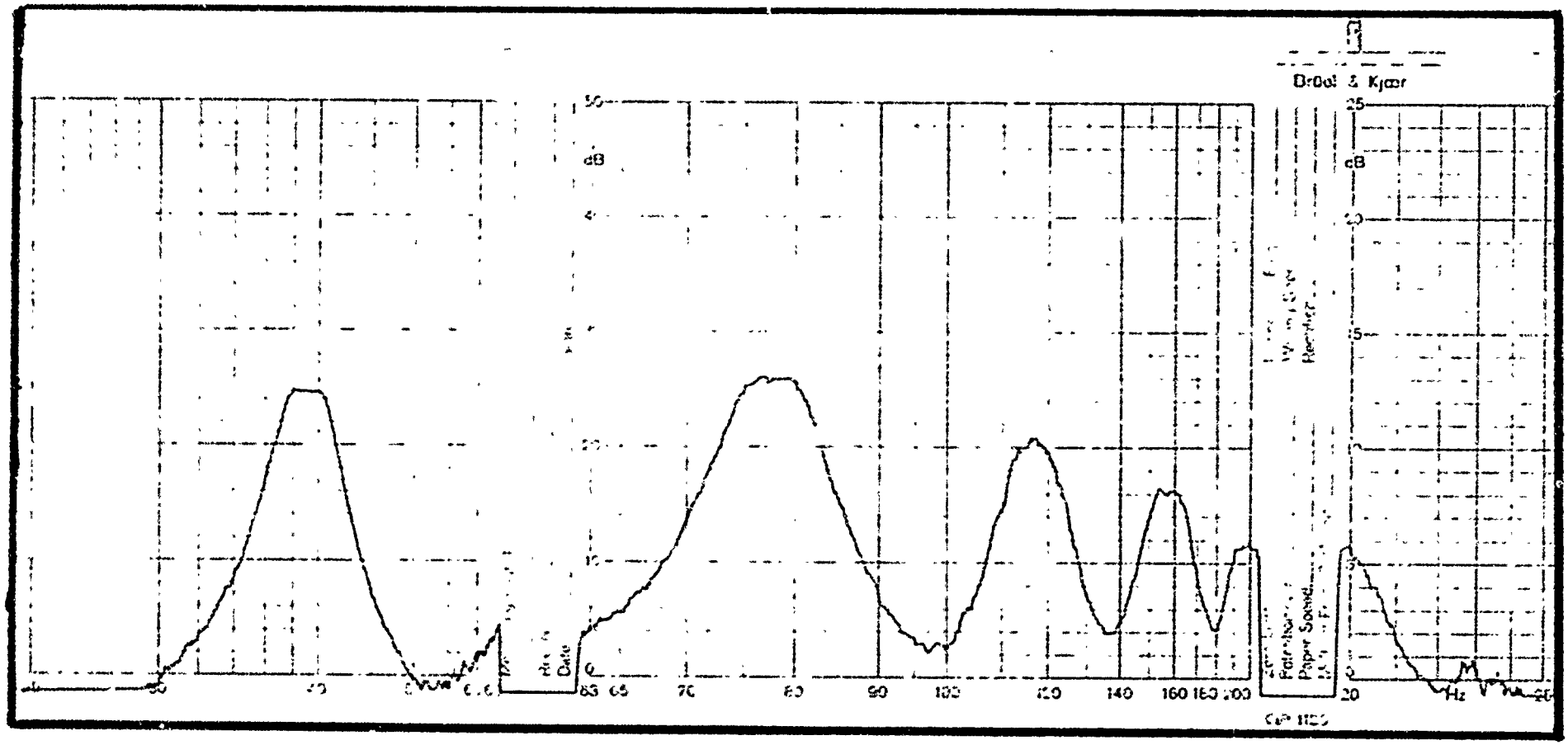

FIGURE 9: SPECTRAL SOUND PRESSURE ANALYSIS FOR THE PROPELLER ALONE

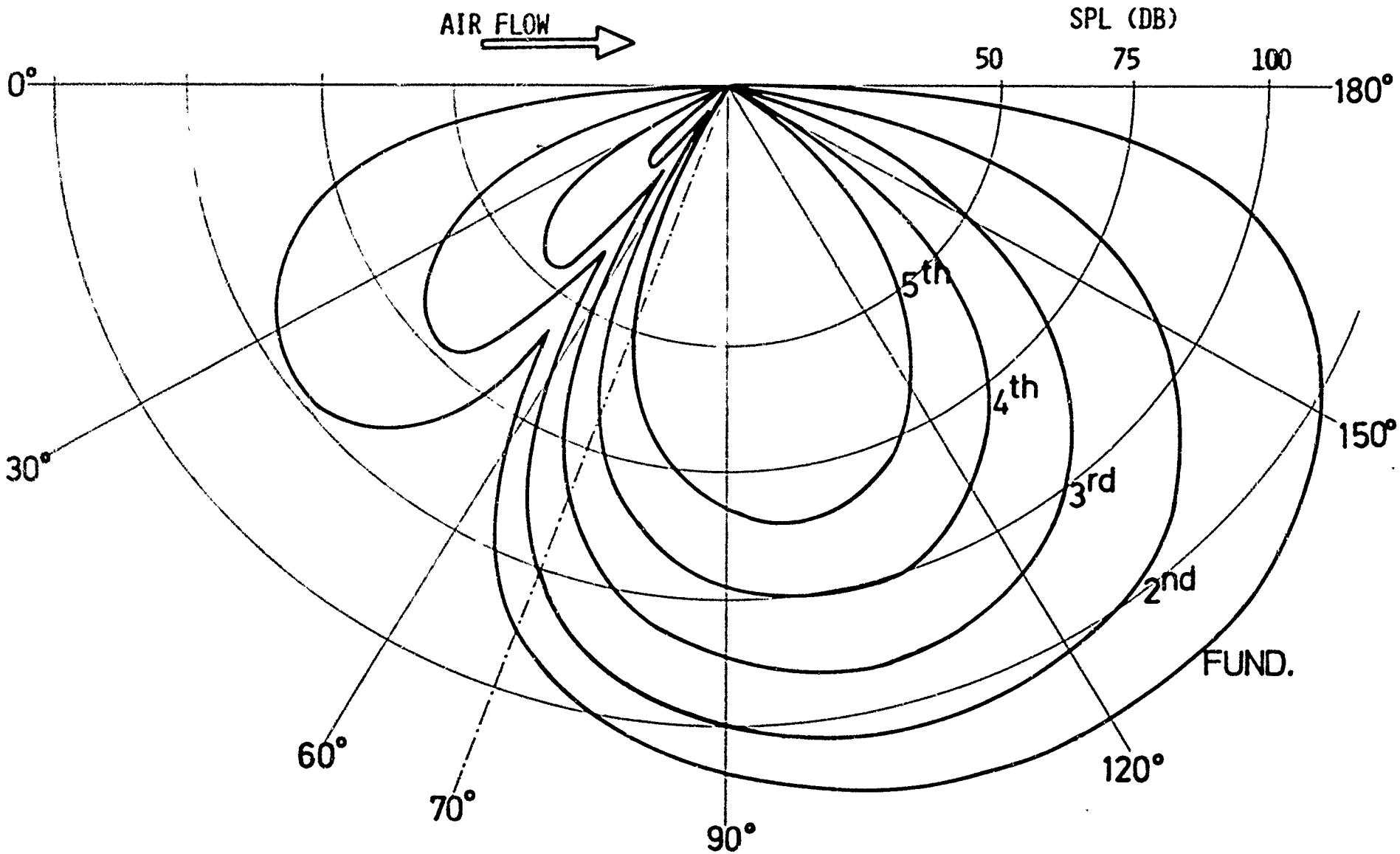

FIGURE 10: THEORETICAL SPECTRAL SOUND PRESSURE LEVELS FOR THE PROPELLER ALONE

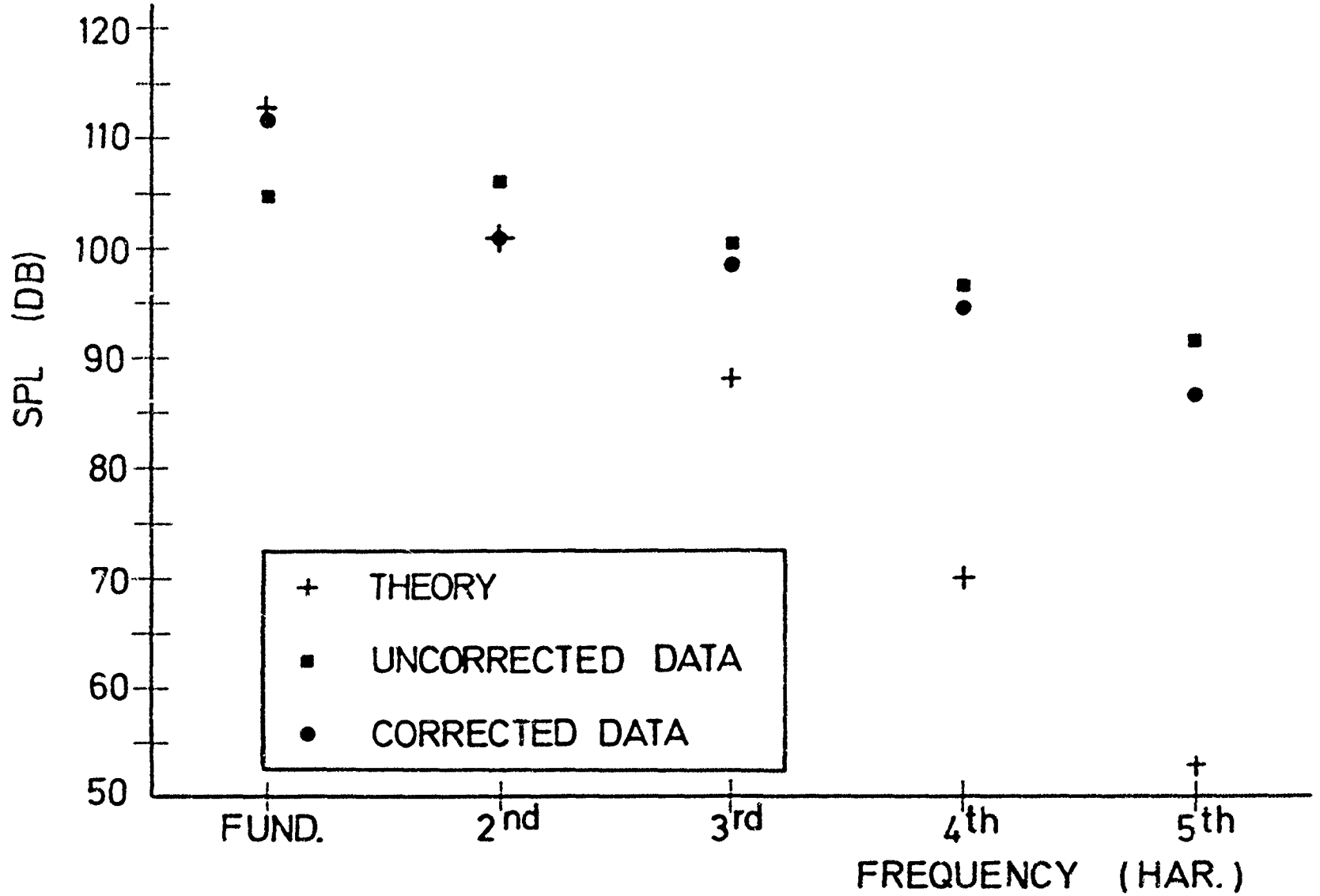

FIGURE 11: THEORETICAL, UNCORRECTED, AND CORRECTED SOUND PRESSURE LEVELS FOR THE PROPELLER ALONE

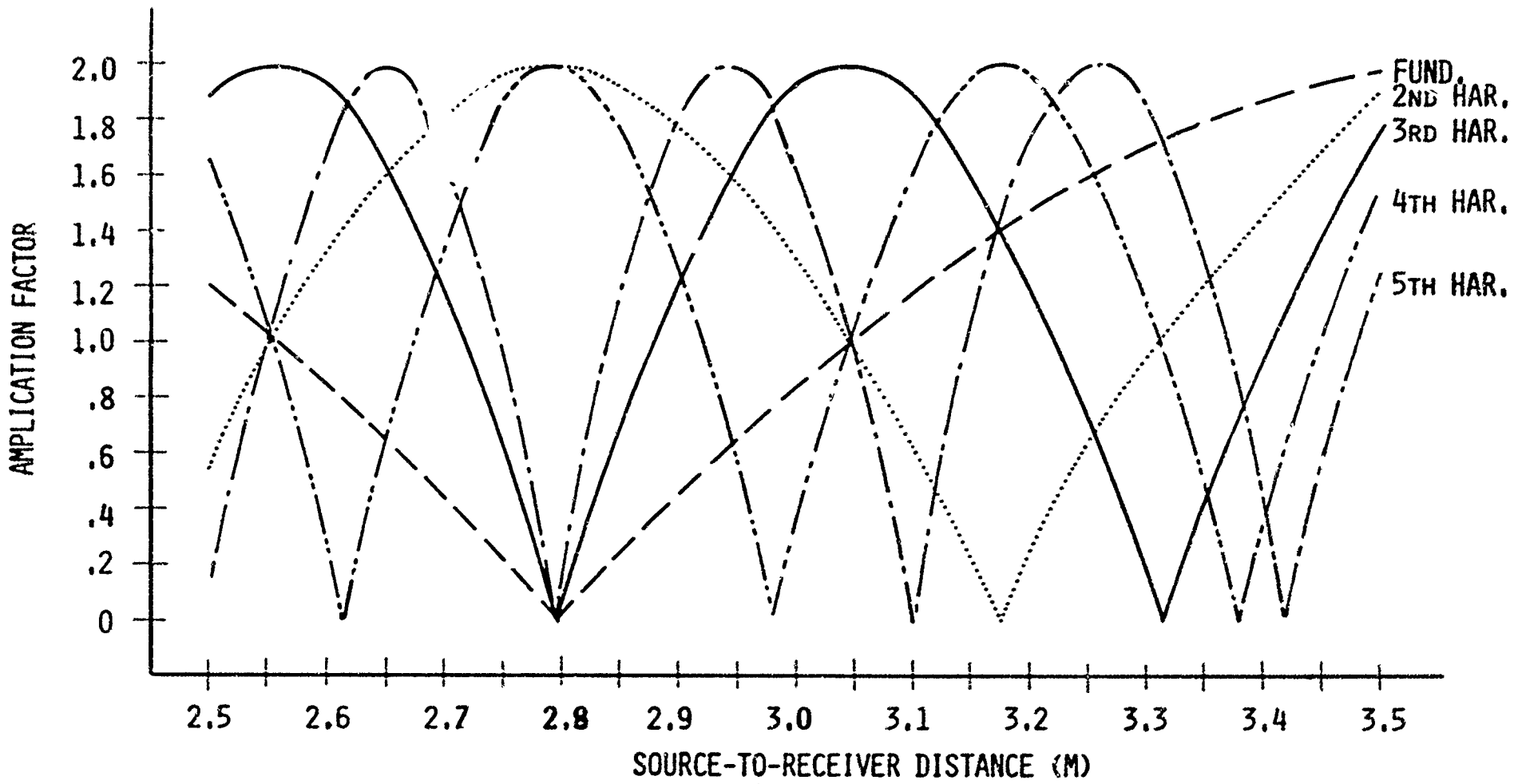

FIGURE 12: AMPLIFICATION FACTORS DUE TO GROUND REFLECTION

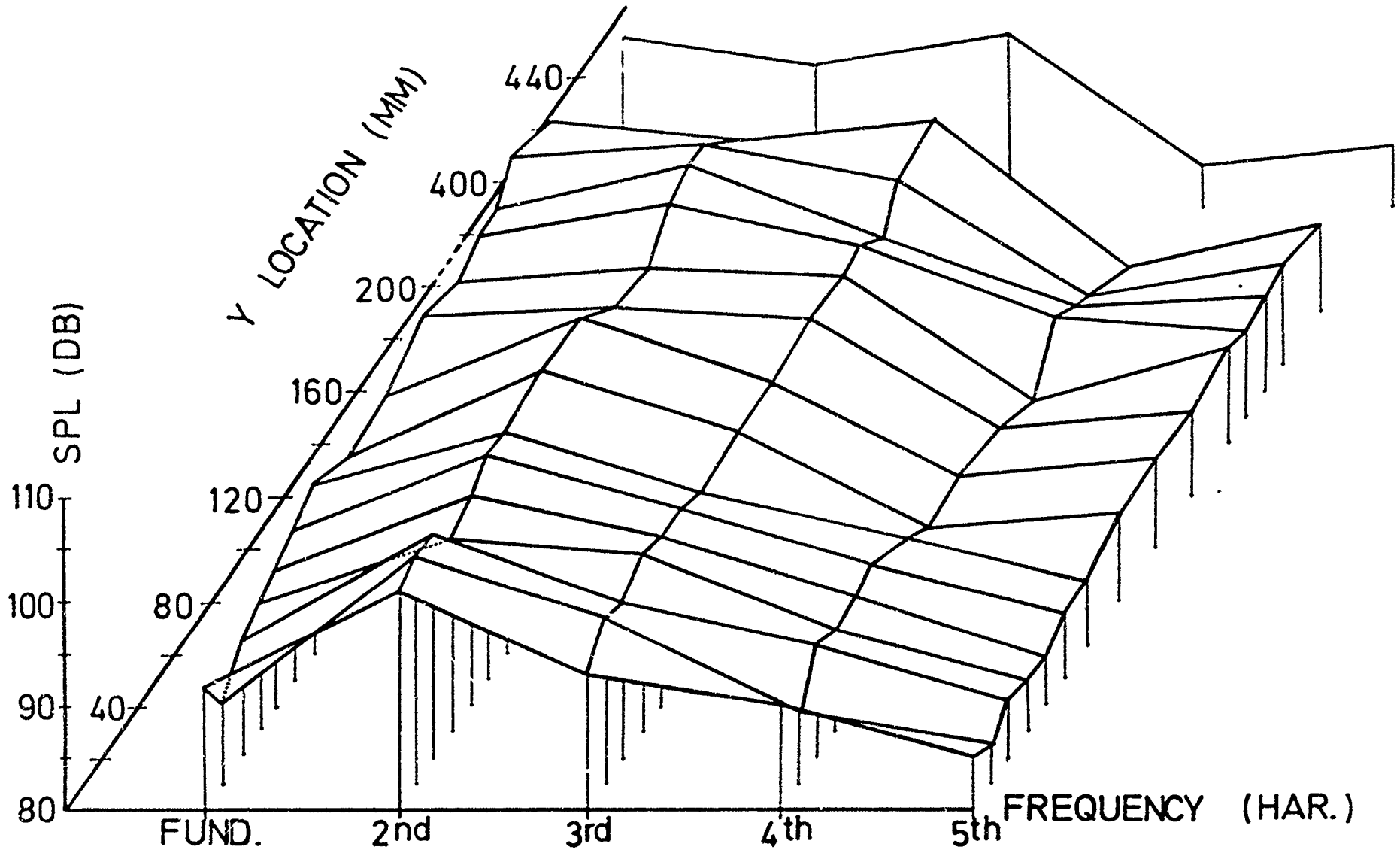

FIGURE 13: UNCORRECTED SOUND PRESSURE LEVELS FOR VARIOUS PROPELLER/WING CONFIGURATIONS

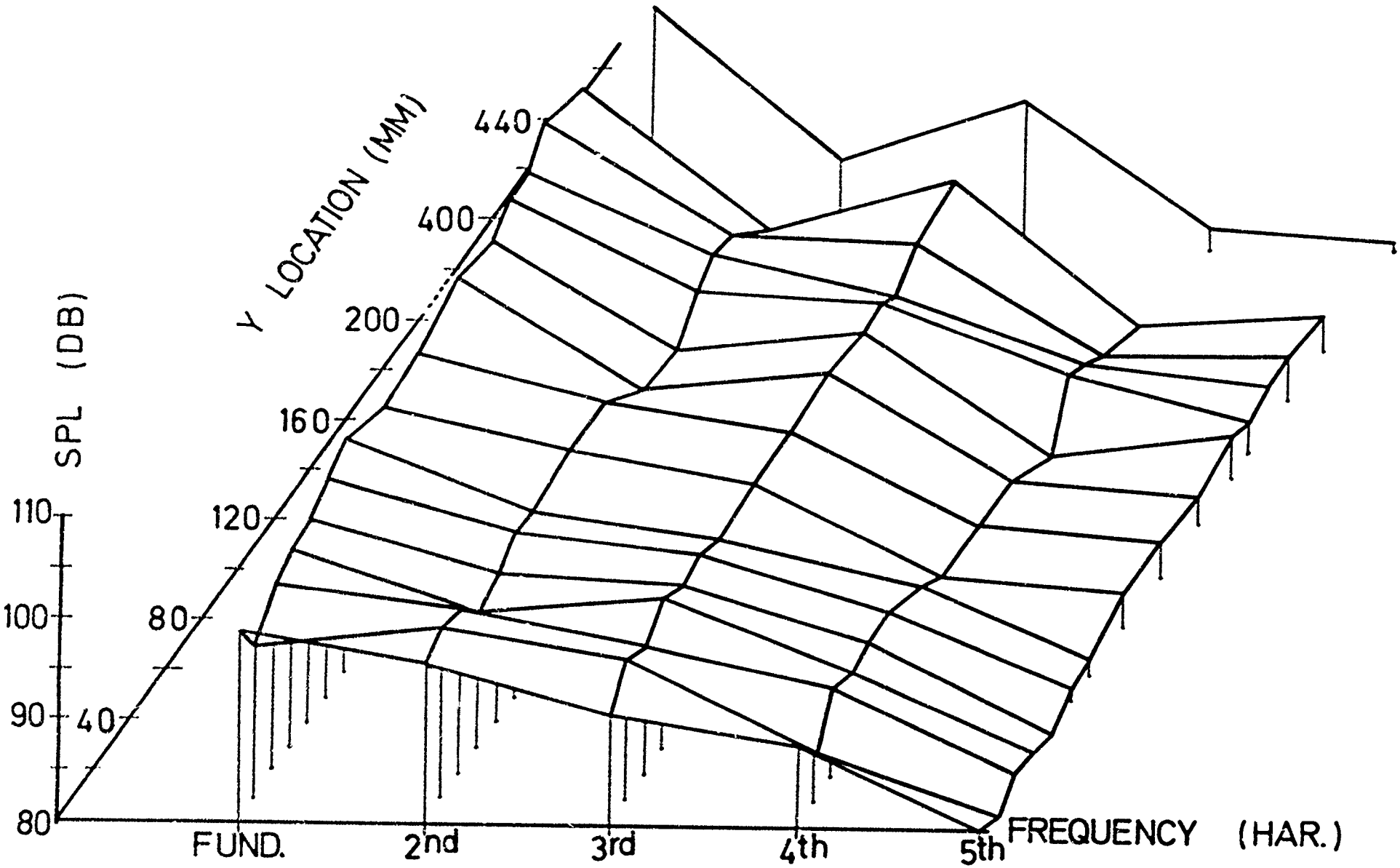

FIGURE 14: CORRECTED SPECTRAL SOUND PRESSURE LEVELS FOR VARIOUS PROPELLER/WING CONFIGURATIONS

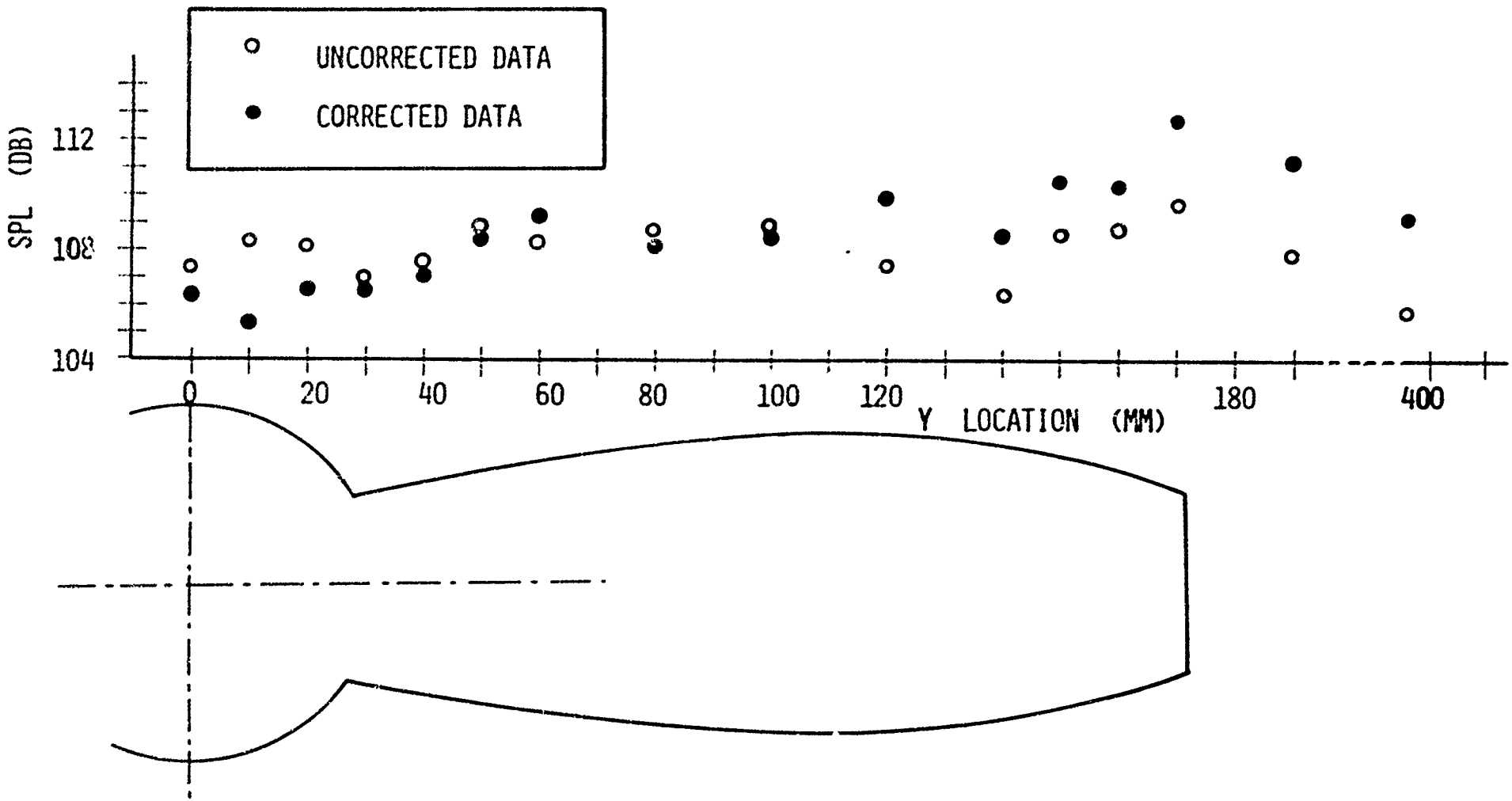

FIGURE 15: OVERALL SOUND PRESSURE LEVELS FOR VARIOUS PROPELLER/WING CONFIGURATIONS